

Spectral Quality Requirements for Effluent Quantification*

R. N. Czerwinski[†]
K. E. Farrar
M. K. Griffin
J. P. Kerekes

Sensor Technology and System Applications Group
Lincoln Laboratory, Massachusetts Institute of Technology
244 Wood Street Lexington, MA 02421
[†]email: rnc@ll.mit.edu tel: 781-981-3924 fax: 781-981-7271

Abstract

Based on simulated atmospheric and sensor effects, we identify spectral resolution and per-channel signal-to-noise ratio (SNR) requirements for thermal infrared spectrometers that allow effluent quantification to any desired precision. This work is based on the use of MODTRAN-4 to explore the effects of temperature contrast and effluent concentration on the spectral slopes of particular absorption features. These slopes can be estimated from remotely sensed spectral data by use of least-squares techniques. The precision of these estimates is based on two factors related to spectral quality: the number of spectral samples that lie along an absorption feature and the radiometric accuracy of the samples themselves. The least-squares process also calculates the slope estimation error variance, which is related to the effluent quantification uncertainty by the same function that maps the slope itself to effluent quantity. The effluent quantification precision is thus shown to be a function of the spacing between spectral channels and the per-channel SNR.

The relationship between SNR, channel spacing and effluent quantification precision is expressed as an equation defining a surface of constant "difficulty." This surface can be used to evaluate parameter sensitivities of sensors in design, to appropriately task sensors, or to evaluate effluent quantification tasks in terms of feasibility.

1. Introduction

Long-wave infrared (LWIR) spectroscopy is being developed as a technology for remote site characterization because it offers a day/night capability to sense the relatively unique material signatures associated with mineral surfaces [1], atmospheric gases [2], and effluent chemicals [3]. In particular, effluent gases such as those associated with industrial activity are well characterized by their LWIR absorption features [4], and can be sensed in quantities useful in environmental monitoring [5] or treaty verification applications [6].

* This work was sponsored by the Department of Defense under Contract F19628-00-C-0002. Opinions, interpretations, conclusions and recommendations are those of the authors and not necessarily endorsed by the United States Government.

To investigate the capability of LWIR sensing, imaging spectrometers have been constructed and test campaigns are underway [5, 7]. Fundamentally, however, imaging spectroscopy involves a trade-off between system parameters that must be optimized for specific tasks. For example, a system designer may have a requirement to quantify a certain material with a minimum uncertainty, and may choose to meet that requirement by specifying the sensor's spectral resolution. This choice may limit the integration time possible, which constrains the sensor's feasible signal-to-noise ratio (SNR). This paper attempts to quantify the effect of those trades for the task of effluent gas quantification.

Specifically, we identify three parameters of interest in sensor design: the number of spectral channels in the 8 – 13 micron band, the per-channel SNR and the quantification uncertainty permitted. We explore the trade space spanned by these parameters and identify sensor operating points within that space (i.e., effluent quantification uncertainties characteristic of a sensor with given number of channels and per-channel SNR). Quantification uncertainty is calculated as the standard deviation of a quantity estimate, and has the same units as quantity: ppm-m-K, the product of effluent concentration (in parts per million), plume thickness (in meters) and temperature contrast (in Kelvin), parameters generally inseparable from a single-view image. It is calculated by a least squares estimation of the slope of an absorption line. These sensor operating points are fit to a plane of constant spectral quality; this plane can be used to evaluate parameter sensitivities of sensors in design, to appropriately task sensors, or to evaluate effluent quantification tasks in terms of feasibility.

2. Effluent Remote Sensing using LWIR HSI

The phenomenon [8] exploited by LWIR spectroscopy is thermal energy radiated or reflected by the surface of the earth or by overlying clouds or gas plume. The contribution of solar illumination is negligible (even in day-time sensing), except to the extent that it warms the earth's surface. Figure 1 shows the major terms that contribute to the radiance measured by the sensor.

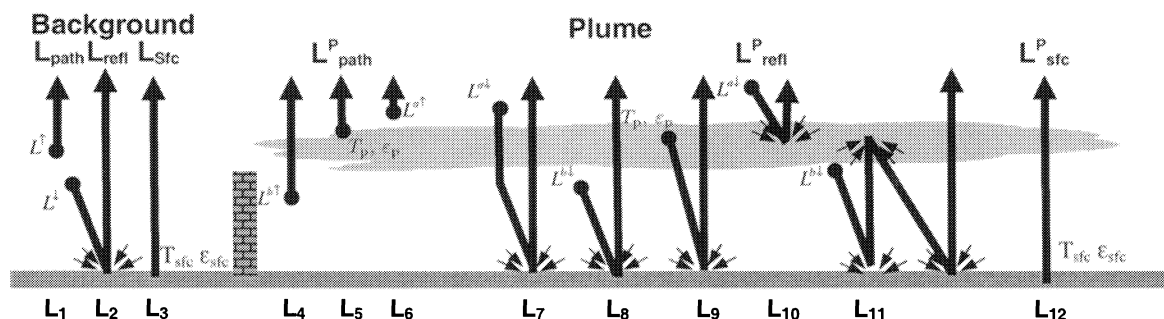


Figure 1: Contributions to sensor radiance in both the presence and absence of an effluent plume.

The figure shows the radiance from two regions, one clear of plume gases, and another in which contributions from near the surface are affected by plume absorption and emission. We will be assuming that for each plume pixel identified, a background spectrum will also be available to provide a contrasting signature; identification of such spectra is an ongoing area of research [4]. The difference between the plume and the background pixel will be called the differential radiance (ΔL), and can be written in terms of the contribution of the twelve components shown in Figure 1. These components will be considered in groups and discussed below.

The first group to be considered is the path radiance, designated L_1 , L_4 , and L_6 . In this treatment, we will assume that the plume lies close to the surface and that little of the path radiance originates below the plume, hence $L_4 = 0$ and $L_1 = L_6$. The contribution of these terms to the differential radiance is thus ignored:

$$\Delta L_{\text{path}} = 0.$$

The second group to be considered is the reflected components, L_2 , L_7 , L_8 , L_9 , L_{10} , and L_{11} . Two of these components, L_8 , and L_{11} are reflected path radiance originating below the plume, and are negligible because the plume lies close to the surface. The L_{10} term (reflected off the plume) is generally very small as well [9] and will also be neglected. The remaining terms are L_2 , L_7 , and L_9 , representing energy reflected off the ground. The differential plume radiance contribution from these terms is

$$\Delta L_{\text{refl}} = L_7 + L_9 - L_2.$$

The final group to consider is the surface radiance, which is usually the most significant radiance received at the sensor. The radiance difference from the surface due to an overlying plume is

$$\Delta L_{\text{sfc}} = L_{12} - L_3.$$

The total radiance difference is obtained by combining these terms and adding the plume radiance (L_5):

$$\begin{aligned} \Delta L &= L_{\text{plume}} + \Delta L_{\text{path}} + \Delta L_{\text{refl}} + \Delta L_{\text{sfc}} \\ &= L_5 + L_7 + L_9 + L_{12} - L_2 - L_3. \end{aligned}$$

Evaluating each term [9], and combining common factors the radiance difference can be approximated by:

$$\begin{aligned} \Delta L &= t_a (1 - t_p) \left\{ B(T_p) - \varepsilon_{\text{sfc}} B(T_{\text{sfc}}) \right. \\ &\quad \left. + (1 - \varepsilon_{\text{sfc}}) [B(T_p) t_p - (1 + t_p) L^{\text{a}\downarrow}] \right\} \\ &\cong t_a (1 - t_p) [B(T_p) - \varepsilon_{\text{sfc}} B(T_{\text{sfc}})] \end{aligned}$$

where $B(T)$ denotes the Planck radiance function:

$$B(T) = \frac{c_1}{\lambda^5 \left[\exp\left(\frac{c_2}{\lambda T}\right) - 1 \right]}$$

written in terms of constants¹ $c_1 = 1.191 \times 10^{11}$, and $c_2 = 1.439 \times 10^4$. The approximation results from neglecting the reflected downwelling components (L_7 , L_9 , and L_2). This is reasonable since surface emissivities are generally above 0.9 [10], which leads to very little reflected downwelling energy in the LWIR. The resulting differential radiance is the product of three terms, one related to the atmospheric transmission, one related to the plume absorption, and one arising from the plume/surface apparent temperature contrast.

If the background has a smooth emissivity, the effect of the surface can be combined into a single apparent temperature function, and expressed as a linearization of the Planck function evaluated at the surface temperature \hat{T}_s multiplied by a plume/temperature difference term ΔT :

$$\begin{aligned} \Delta L &= \{B(T_p) - B(T_s)\varepsilon_s\} (1 - t_p)t_a \\ &= \{B(T_p) - B(\hat{T}_s)\} (1 - t_p)t_a \\ &\approx \Delta T_p \left. \frac{\partial B(T)}{\partial T} \right|_{T=\hat{T}_s} (1 - t_p)t_a \end{aligned}$$

The effect of the plume is a term of the form $(1 - t_p)$, which can then be approximated for optically thin plumes (small optical depths) using a linearization of the Beer-Lambert equation:

$$\begin{aligned} 1 - t_p &= 1 - e^{-a(\lambda)CL} \\ &= 1 - \left[1 - a(\lambda)CL + \frac{1}{2!} (a(\lambda)CL)^2 - \dots \right] \\ &\approx CLa(\lambda) \end{aligned}$$

where C is the concentration of the effluent in the plume, L is the path length of plume observed by the sensor and $a(\lambda)$ is the absorption coefficient characteristic of the gas. An approximation for the radiance difference is then obtained by combining terms:

$$\begin{aligned} \Delta L &\approx CL\Delta T_p a(\lambda) \left. \frac{\partial B(T)}{\partial T} \right|_{T=\hat{T}_s} t_a \\ &\approx K(\lambda)CL\Delta T_p a(\lambda) \end{aligned}$$

where $K(\lambda)$ is given by

¹ Constants normalized such that λ is expressed in microns.

$$K(\lambda) = \left. \frac{\partial B(T)}{\partial T} \right|_{T=T_s} t_a$$

a function of wavelength which includes surface and atmospheric effects. This is a smooth function whose effect on quantification algorithms can be compensated. To a first order approximation, the (compensated) radiance difference between a plume pixel and a background pixel is directly proportional to the product of plume concentration, thickness and temperature contrast and to the absorption signature of the plume constituent. In the next section, we use MODTRAN-4 to calculate high resolution expected radiance difference spectra, suitable for evaluation within a parameter space of sensor configurations being considered for an effluent quantification task.

3. Signature Modeling with MODTRAN

To generate high-spectral resolution (4 cm^{-1}), noise-free radiances free of sensor artifacts, MODTRAN-4 [11] was used to calculate at-sensor radiances for a variety of concentrations and temperature contrast values. Attention was focused on SO_2 because of its wide absorption feature near 8.62 microns. The MODTRAN-4 runs include the effects characteristic of nadir view remote sensing from the lower stratosphere (18 km altitude) through a mid-latitude summer atmosphere, and assume a featureless surface with 97% emissivity and constant temperature of 295K. The plume is assumed to be 10 meters thick, to lie 20-30 meters above the surface, and to be surrounded by ambient air at 294K.

The plume itself is varied from run to run, over a matrix of temperatures and concentrations. The radiance differences due to the plume for several parameter excursions are plotted in Figure 2. In each panel, the solid curve represents a “nominal” radiance difference, corresponding to a concentration of 10^{19} molecules per cm^2 and temperature 10K above that of the ambient air. The left panel shows two excursions in concentration (factor of 10 above and below the nominal), and the right panel shows two excursions in temperature (10K above and below the nominal). The limits of the excursions were selected to sample the dynamic range of observable radiance differences, while avoiding concentrations that result in optically thick plumes, where the linear relationship between absorption and concentration breaks down.

The slope of the absorption line is clearly related to both the concentration and temperature of the plume, as predicted by the radiative transfer analysis of the previous section. Figure 3 shows the slope of the SO_2 absorption feature measured near 9.1 microns as a function of plume “quantity” – the product of plume concentration, thickness and temperature contrast which has units of ppm-m-K. Each marker on the plot represents the slope of an absorption feature extracted from a single MODTRAN-4 run. Note that markers corresponding to negative temperatures (i.e. plume cooler than background) correspond to negative slopes. This is expected behavior for a plume demonstrating an absorption (rather than emission) feature.

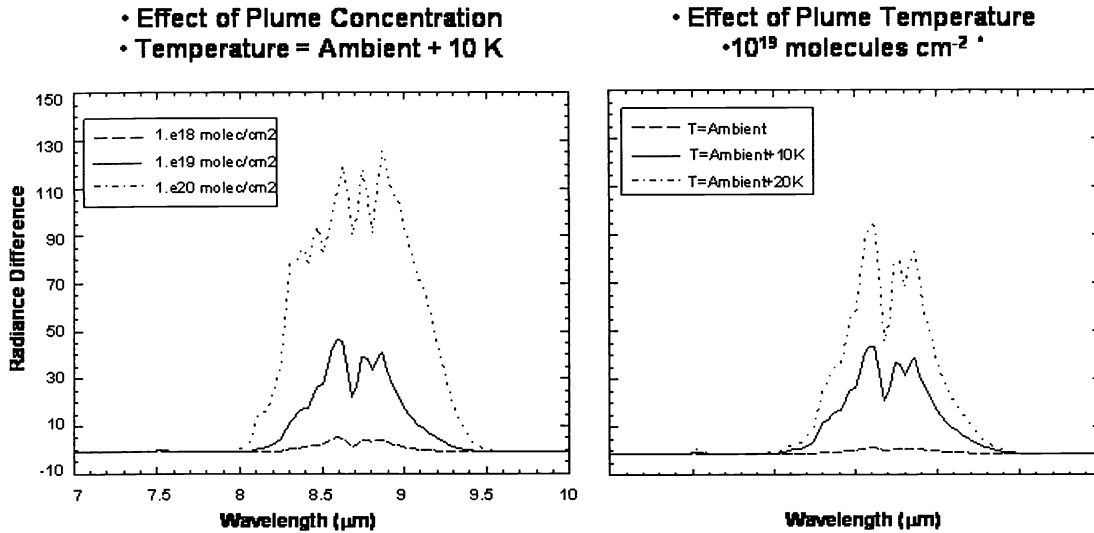


Figure 2: MODTRAN-4 predicted differential radiances. The left plot shows the effect of increased or decreased concentration at constant temperature; the right plot shows the effect of plume temperature.

Figures 2 and 3 reinforce our earlier assertion of an approximately linear relationship between measurable absorption slope and the “quantity” we wish to estimate. It also demonstrates a linear relationship between slope measurement *errors* and errors in estimation of plume quantity. In the next section, slope measurement will be carried out through least-squares estimation, and the statistical slope error will be mapped to statistical quantification error through this linear relation.

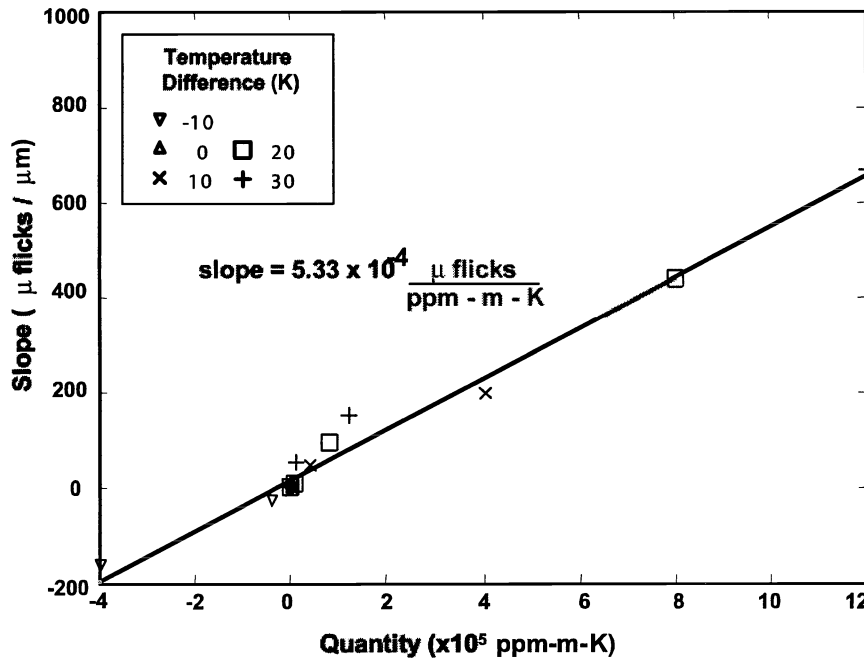


Figure 3: The slope of the SO₂ absorption feature at 9 microns estimated from MODTRAN-4 runs with a simulated plume of varying concentration and thickness.

4. A Least-Squares Approach to Effluent Quantification

This section describes the least-squares estimation of the slope of an absorption feature, which has previously been shown to be related to the problem of effluent quantification. We make no claims about the optimality of this approach; it is used here because it permits an error analysis useful for the parameter studies used later to assess spectral quality².

Assuming the absorption feature has the functional form of a line, the matrix representation of the feature is:

$$y = \begin{bmatrix} 1 \\ x \\ \vdots \\ 1 \end{bmatrix} \begin{bmatrix} m \\ b \end{bmatrix} = A \begin{bmatrix} m \\ b \end{bmatrix},$$

where x is a vector of the wavelengths which lie along the absorption feature, y is the measured radiance difference measured at each wavelength, and m and b are slope and intercept values to be estimated. The dimensionality of the vectors is the number of samples which lie on the feature of interest, and is thus related to sensor spectral resolution and feature size.

The parameter estimate is performed using a least-squares matrix inverse:

$$\begin{bmatrix} \hat{m} \\ \hat{b} \end{bmatrix} = (A^T A)^{-1} A^T (y + n) \quad \text{where } n : N(0, \Sigma)$$

Note that this equation explicitly shows the effect of sensor noise n on the slope and intercept estimates. This is shown as a Gaussian distribution, but this assumption is required only to simplify the closed form error estimate derived below.

The slope and intercept estimates are themselves random quantities, with mean and covariance which can be written in terms of the sensor noise mean and covariance. If sensor noise is zero mean, the slope and intercept estimates will be unbiased,

$$\varepsilon = \begin{bmatrix} m - \hat{m} \\ b - \hat{b} \end{bmatrix} = (A^T A)^{-1} A^T (y + n) - \begin{bmatrix} m \\ b \end{bmatrix} = 0$$

but have the following covariance:

$$E[\varepsilon \varepsilon^T] = (A^T A)^{-1} A^T \Sigma A (A^T A)^{-1}$$

² While adequate for effluents with broad absorption features, it would not be appropriate for effluents with narrow features, like ammonia.

Note that the error covariance is related only to the sensor covariance and the spectral channel spacing, and not on the measurements themselves (though the sensor covariance can be calculated from in-scene statistics if they are available). This property of data independence allows us to use the value of the error covariance matrix to evaluate sensor parameters like channel spacing and SNR in trade studies to assess spectral quality.

5. Spectral Quality Predictions

The error covariance matrix $E[\varepsilon \varepsilon^T]$ is a characterization of the precision with which effluent quantification can be performed. It is related to spectral resolution (through the number and placement of samples used to compute it) and to sensor noise (through the implicit sensor covariance Σ), and can thus be used to identify combinations of sensor parameters which result in similar “quality” of the resulting spectral data. It can also be used to conduct trade studies to demonstrate the relative importance in spectral imaging of parameters such as signal-to-noise ratio and spectral resolution.

The error covariance matrix entry corresponding to the effluent quantification error variance can be calculated by expanding the terms of the least-squares inverse above. While complicated in appearance, the matrix inverse $(A A^T)^{-1}$ is a 2×2 matrix with no rank deficiencies and its entries can be calculated in the form of sums of terms. The quantification error variance (i.e. the upper left entry of $E[\varepsilon \varepsilon^T]$) can be written as follows:

$$\sigma_m^2 = \frac{2N_L \sum x_i^2 \sigma_i^2 + 2 \left(\sum x_i^2 \right) \left(\sum \sigma_i^2 \right) - 4N_L \left(\sum x_i \right) \left(\sum x_i \sigma_i^2 \right)}{N_L \left(\sum x_i^2 \right) - \left(\sum x_i \right)^2}$$

where N_L is the number of spectral channels which lie along the feature to be estimated, x_i is a wavelength along the slope, and σ_i is the sensor noise (in micro-flicks³) on the i th channel. Assuming the spectrometer has N equally spaced samples between 8 and 13 microns, and equal per channel noise σ , and that the spectral feature is W microns wide, the sums above can be simplified into closed form as

$$\sigma_m^2 = \frac{120\sigma^2 N}{W [W^2 N^2 - 25]}.$$

This expression can be used to infer relationships between sensor parameters N and σ , and the achievable slope precision σ_m . This slope precision is related to effluent quantification uncertainty by the slope of the fit line shown in Figure 3:

$$\sigma_Q^2 = \left[\frac{1 \text{ppm} - m - K}{5.33 \times 10^{-4} \mu\text{flicks}/\mu\text{m}} \right]^2 \frac{120\sigma^2 N}{W [W^2 N^2 - 25]}.$$

This equation is used in Figure 4 to calculate the quantification uncertainty as a function of sensor noise for four different levels of spectral resolution. For any given sensor

³ One microflick is $1 \mu\text{W}/\text{cm}^2 \text{ sr } \mu\text{m}$

configuration, increasing noise directly adds to the uncertainty of effluent quantification. Note that sensor noise as used here is independent of spectral resolution. In other words, reducing the number of channels does not improve sensor SNR through either improved signal or reduced noise.

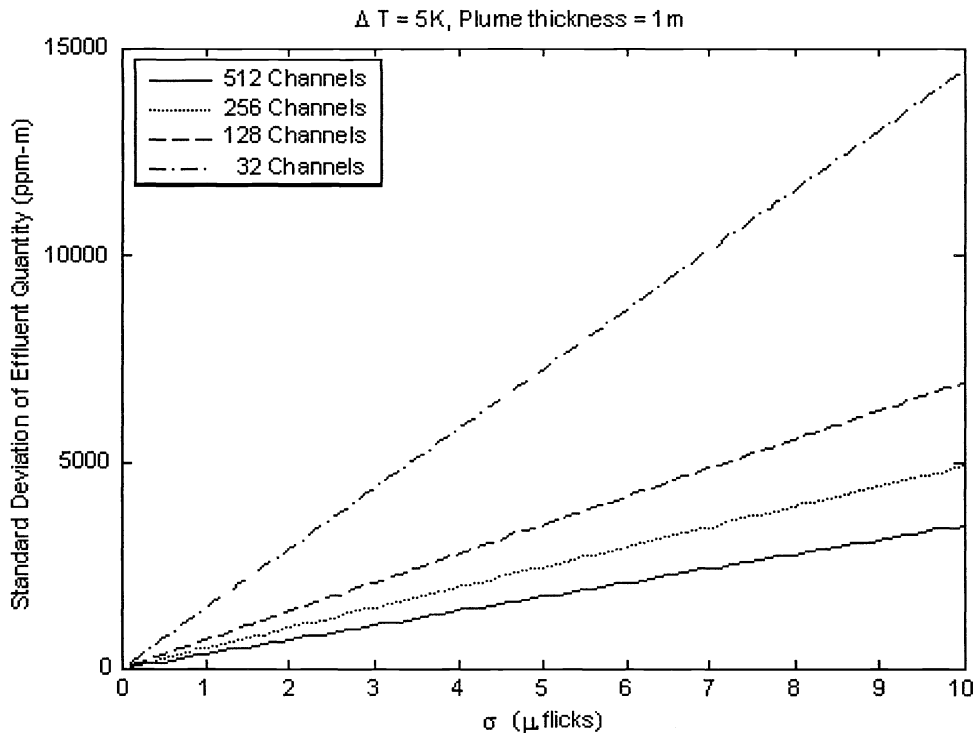


Figure 4: Effluent quantification precision possible as a function of per-channel sensor noise, calculated for four different resolution spectrometers.

Figure 5 shows quantification uncertainty as a function of the number of channels for four different sensor noise levels. The behavior of these curves indicates a threshold effect, where increasing the number of channels past a certain point leads to diminishing improvement in effluent quantification accuracy. This is a result of the estimation procedure: once spectral resolution has reached a point where several data points lie along an absorption line, further increases in resolution do not help to improve an already good slope estimate. Conversely, as the number of channels is reduced, eventually the sensor capability is reduced to the point where too few measurements are made along the absorption line and no slope estimate can be achieved. This is the reason why the curves in Figure 5 cut off at approximately 25 channels.

These curves are slices through a spectral quality surface, which consists of parameter combinations that lead to similar sensor performance. Figure 6 shows the points plotted as a surface. Note that the axes have been log transformed, and sensor noise has been transformed by a reciprocal (now proportional to signal to noise ratio, with proportionality constant incorporated without loss of generality into the constant K). With these transformations, the plane of the surface is evident; the equation of this spectral quality surface is

$$SQRS = K + 0.13 \log N + 0.26 \log SNR + 0.26 \log \sigma_o$$

This equation is expressed in a style reminiscent of the General Image Quality Equation [12, 13], developed to assist in assessing quality of EO imagery.

It should be noted that this equation is useful mainly to infer general relationships between sensor parameters, not to imply specific performance capability. Hence, the uncertain value of the constant K is not a significant limitation on the utility of this work. Indeed, evaluation of the K would require a demonstration of effluent quantification to known precision using a well characterized spectrometer, which is presently unavailable. Thus, the development of a rating scale for effluent quantification tasks in the style of [12,13] is not presently feasible. Nevertheless, certain relationships can be observed from the SQRS equation. For example, the 2:1 ratio between the coefficients corresponding to SNR and spectral resolution indicate the relative importance of those parameters, which is consistent with other published work on LWIR spectral utility such as that presented in [3].

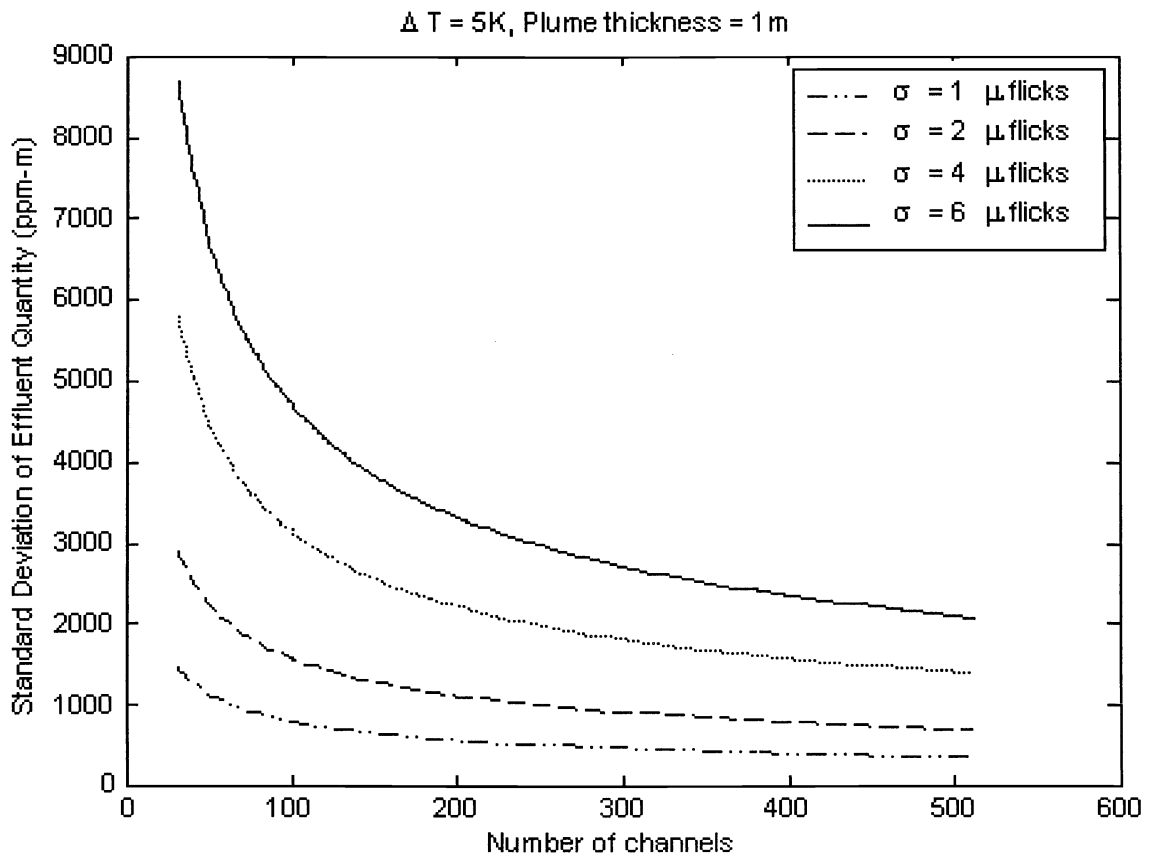


Figure 5 Effluent quantification precision possible as a function of per-channel sensor noise, calculated for four different sensor noise levels.

6. Summary

This paper has reviewed the motivation for the derivation of a spectral quality metric appropriate for effluent quantification and other remote sensing tasks. We have derived approximate expressions for the observable signature of an effluent plume and showed that to first order, an optically thin plume's signature is linearly related to its concentration, thickness and temperature contrast, three factors generally inseparable from a single-view remote measurement.

We have also shown through MODTRAN-4 runs the atmospherically modified at-sensor radiance observable over a range of plume scenarios, and showed an approach to quantification based on least-squares estimation of an absorbance slope. This technique leads to estimation errors that can be statistically characterized as functions of sensor parameters. The estimation error is used to identify specific parameter trades that lead to similar sensor performance (for effluent quantification); these points are shown to lie on a surface that can be used to interpolate to other points of similar spectral quality.

Much future work remains in the areas of developing spectral quality approaches to other LWIR exploitation tasks, such as detection and identification of effluent material.

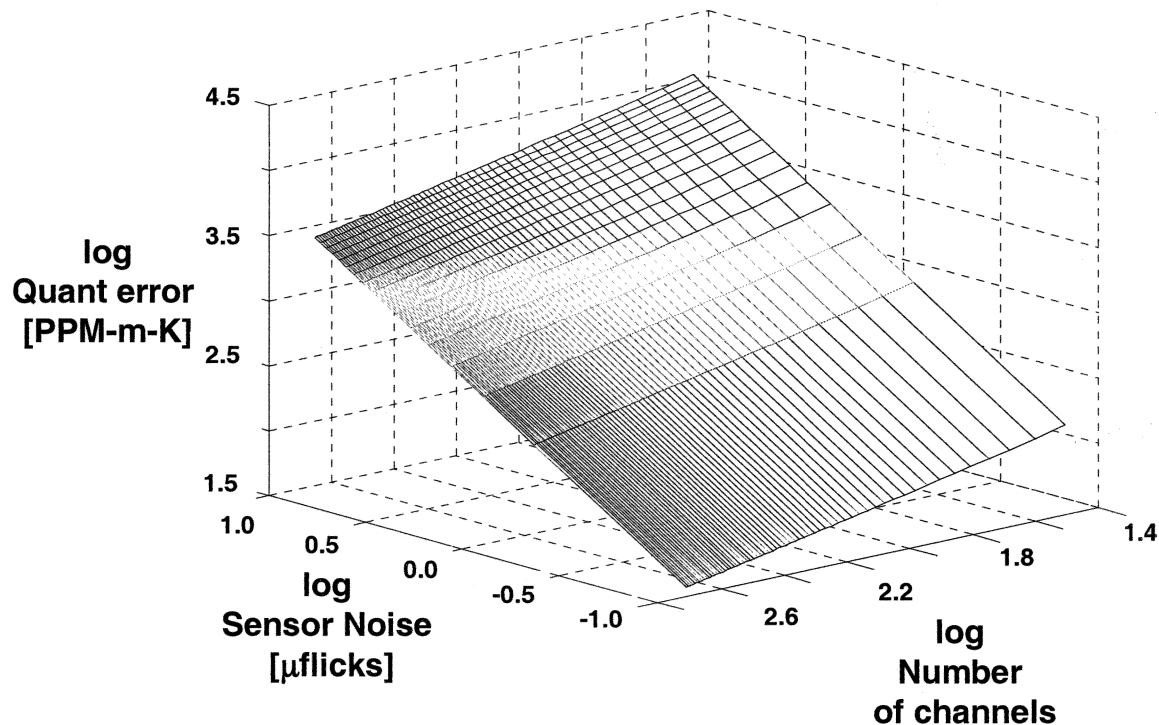


Figure 6: Spectral quality surface corresponding to equivalent sensor-performance parameter triplets identified in Figures 4 and 5.

7. References

- [1] L. E. Kirkland, K. C. Herr and J. W. Salisbury, "Thermal Infrared Spectral Band Detection Limits for Unidentified Surface Materials," *Applied Optics*, May 2001.
- [2] E. D. Hernandez-Baquero and J. R. Schott, "Atmospheric and Surface Parameter Retrievals from Multispectral Thermal Imagery via Reduced-rank Multivariate Regression," *Proceedings IEEE IGARSS 2000*, 24-28 July 2000, pp 1525 – 1527.
- [3] J. S. Margolis, K. Y. Liu and P. I. Moynihan, "Spectroscopic Observations of Low-lying Gas Clouds: Sensitivity of Detection by Method of Covariance Matrix," in *Air Monitoring and Detection of Chemical and Biological Agents*, Joseph Leonelli, Mark L. Althouse, Editors, Proceedings of SPIE, vol. 3533, pp 25-32 (1999).
- [4] Young, S. J., "Detection and Quantification of Gases in Industrial-Stack Plumes Using Thermal-Infrared Hyperspectral Imaging," Aerospace Project Report No. ATR-2002(8407)-1, The Aerospace Corporation, El Segundo, CA. Available at www.aero.org
- [5] J. J. Szymanski et al, "MTI Science, Data Products, and Ground-Data Processing Overview," in *Algorithms for Multispectral, Hyperspectral, and Ultraspectral Imagery VII*, Sylvia S. Shen, Michael R. Descour, Editors, Proceedings of SPIE, vol. 4381, pp. 195-203 (2001).
- [6] R. R. Kay, "Multispectral Thermal Imager (MTI) Payload Overview," in *Imaging Spectrometry V*, Michael R. Descour, Sylvia S. Shen, Editors, Proceedings of SPIE, vol 3753, pp 347-358 (1999).
- [7] J. A. Hackwell et al., "LWIR/MWIR Imaging Hyperspectral Sensor for Airborne and Ground-based Remote Sensing," in *Imaging Spectrometry II*, Michael R. Descour, Jonathan M. Mooney, Editors, Proceedings of SPIE, vol. 2819, pp 102-107 (1996).
- [8] J. P. Kerekes et al., "Modeling of LWIR Hyperspectral System Performance for Surface Object and Effluent Detection Applications," in *Algorithms for Multispectral, Hyperspectral, and Ultraspectral Imagery VII*, Sylvia S. Shen, Michael R. Descour, Editors, Proceedings of SPIE Vol. 4381, pp. 348-359 (2001).
- [9] M. K. Griffin et al., "Characterization of gaseous effluents from modeling of LWIR hyperspectral measurements," in *Algorithms for Multispectral, Hyperspectral, and Ultraspectral Imagery VII*, Sylvia S. Shen, Michael R. Descour, Editors, Proceedings of SPIE Vol. 4381, pp 360-369 (2001).
- [10] M. K. Griffin, private communication.
- [11] A. Berk et al., "MODTRAN Cloud and Multiple Scattering Upgrades with Application to AVIRIS," *Remote Sens. Environ.*, 65:367 – 375 (1998).
- [12] J. C. Leachtenauer et al., "General Image-Quality Equation: GIQE," *Applied Optics*, vol. 36, No. 32, 10 November 1997, pp. 8322-8328.
- [13] J. C. Leachtenauer et al., "General Image-Quality Equation for infrared imagery," *Applied Optics*, vol. 39, No. 26, 10 September 1997, pp. 4826-4828